Queensland University of Technology
Brisbane Australia

This is the author's version of a work that was submitted/accepted for publication in the following source:

Liu, F., Zhuang, P., & Burrage, K. (2012) Numerical methods and analysis for a class of fractional advection dispersion models. *Computers and Mathematics with Applications*, *64*(10), pp. 2990-3007.

This file was downloaded from: http://eprints.qut.edu.au/51515/

© Copyright 2012 Elsevier Ltd.

Notice: *Changes introduced as a result of publishing processes such as copy-editing and formatting may not be reflected in this document. For a definitive version of this work, please refer to the published source:*

http://dx.doi.org/10.1016/j.camwa.2012.01.020

Numerical methods and analysis for a class of fractional advection-dispersion models

F. Liu [a,*], P. Zhuang [b], K. Burrage [a,c]

[a] *School of Mathematical Sciences, Queensland University of Technology, GPO Box 2434, Brisbane, Qld. 4001, Australia*

[b] *School of Mathematical Sciences, Xiamen University, China*

[c] *Department of Computer Science and OCISB, University of Oxford, OX1 3LB,* UK

Abstract

In this paper, a class of fractional advection-dispersion models (FADMs) is considered. These models include five fractional advection-dispersion models, i.e., the times FADM, the mobile/immobile time FADM with a time Caputo fractional derivative $0 < \gamma < 1$, the space FADM with two sides Riemann-Liouville derivatives, the time-space FADM and the time fractional advection-diffusion-wave model with damping with index $1 < \gamma < 2$. These equations can be used to simulate the regional-scale anomalous dispersion with heavy tails. We propose computationally effective implicit numerical methods for these FADMs. The stability and convergence of the implicit numerical methods are analysed and compared systematically. Finally, some results are given to demonstrate the effectiveness of theoretical analysis.

Key words: Fractional advection-dispersion models, implicit numerical methods, stability, convergence, fractional calculous.

1 Introduction

An advection-dispersion equation (ADE) has commonly been used to describe the Brownian motion of particles [19]. ADE describes the change of probability of a random function in space and time; hence it is naturally used to describe solute transport. The general ADE for the motion of a concentration field

* Corresponding author.
Email address: f.liu@qut.edu.au (F. Liu).

$C(x;t)$ of one space variable x at time t has the form [19]

$$\frac{\partial C(t)}{\partial t} = \left[-V\frac{\partial}{\partial x} + D\frac{\partial^2}{\partial x^2}\right] C(x,t), \tag{1}$$

where $D > 0$ is the diffusion coefficient and $V > 0$ is the drift coefficient. Eq. (1) is a linear second-order partial differential equation of parabolic type.

Dispersion of aqueous tracers in natural systems including heterogeneous soils, aquifers, and rivers, is typically observed to be non-Fickian, also called "anomalous" [23]. Non-Fickian transport behaviour may be due to different mechanisms.

In many studies of diffusion processes where the diffusion takes place in a highly non-homogeneous medium, numerous numerical experiments indicate that anomalous dispersion cannot be described by the traditional second-order ADE without extremely detailed information on the connectivity of high and low hydraulic conductivity sediments [1,3,4,6], it may even be that the ADE is insufficient at any level of detail [10]. The non-homogeneities of the medium may alter the laws of Markov diffusion in a fundamental way. In particular, the corresponding probability density of the concentration field may have a heavier tail than the Gaussian density, and its correlation function may decay to zero at a much slower rate than the usual exponential rate of Markov diffusion, resulting in long-range dependence (LRD). This phenomenon is known as anomalous diffusion [5]. Some researchers have investigated the spatiotemporal nonlocality underlying fractional-derivative models as a possible explanation for regional-scale anomalous dispersion with heavy tails [23]. Some partial differential equations of space-time fractional order were successfully used for modelling relevant physical processes [11].

In this paper, we consider a class of the FADM including the five fractional advection-dispersion models as one special case of these models. The five alternative fractional advection-dispersion models (FADMs) are the times FADM, the mobile/immobile time FADM with a temporal fractional derivative $0 < \gamma < 1$, the space FADM with skewness, both the time and space FADM and the time fractional advection-diffusion-wave model with damping with index $1 < \gamma < 2$, respectively. They describe nonlocal dependence on either time or space, or both, to explain the development of anomalous dispersion. These models have been discussed by Zhang et al. [23] and used to simulate the solute transport in watershed catchments and rivers. However they did not discuss numerical methods and the stability and convergence of these numerical methods in details. The fractional advection-dispersion equations have been recently treated by a number of authors [8,9,13]. It is presented as a useful approach for the description of transport dynamics in complex systems which are governed by anomalous diffusion and non-exponential relaxation patterns. Mainardi, Luchko and Pagnini considered the space-time fractional

diffusion equation and provided a general representation of the Green functions in terms of Mellin-Barnes integrals in the complex plane [12]. Podlubny proposed a general approach to the numerical solution of partial fractional differential equations, which is based on the matrix form representation of discretized fractional operators introduced in [17,18]. However, numerical methods and analysis of stability and convergence for the fractional partial differential equations are quite limited and difficult to derive. This motivates us to consider effective implicit numerical methods, stability and convergence of the implicit numerical methods for a class of fractional advection-dispersion models.

The structure of the remainder of this paper as follows. A class of the fractional advection-dispersion models are considered in Section 2. We propose computationally effective implicit numerical methods for the FADM in Section 3. The stability and convergence of the numerical methods are discussed in Sections 4 and 5, respectively. Finally, numerical examples are given.

2 A class of the fractional advection-dispersion models

In this section we consider the class of the fractional advection-dispersion models (FADMs) [23]:

$$\begin{aligned}\beta_1\frac{\partial C(x,t)}{\partial t}+\beta_2\frac{\partial^\gamma C(x,t)}{\partial t^\gamma}&=-V\frac{\partial C(x,t)}{\partial x}\\ +D(\frac{1}{2}+\frac{q}{2})\frac{\partial^\alpha C(x,t)}{\partial x^\alpha}&+D(\frac{1}{2}-\frac{q}{2})\frac{\partial^\alpha C(x,t)}{\partial(-x)^\alpha}+f(x,t),\end{aligned}\tag{2}$$

with boundary conditions:

$$C(a,t)=\phi_1(t),\quad C(b,t)=\phi_2(t),\quad 0\le t\le T,\tag{3}$$

and initial conditions: when $0<\gamma\le 1$

$$C(x,0)=\varphi_0(x),\quad a\le x\le b,\tag{4}$$

and when $1<\gamma\le 2$

$$C(x,0)=\varphi_0(x),\quad \frac{\partial C}{\partial t}=\varphi_1(x),\quad a\le x\le b,\tag{5}$$

where $\beta_1\ge 0$, $\beta_2\ge 0$, $|\beta_1|+|\beta_2|\ne 0$, $-1\le q\le 1$, $1<\alpha\le 2$, $V>0$, $D>0$ and $0<\gamma\le 2$ are unknown parameters; V is the drift of the process, that is, the mean advective velocity, D is the coefficient of dispersion; q indicates the relative weight of forward versus backward transition probability. The most

frequently encountered definition of fractional derivatives are the Caputo and the Riemann-Liouville derivatives.

Definition 1. For functions $C(x,t)$ given in the interval $[0,T]$, the expressions [9,16]

$$D_t^\gamma C(x,t) = \begin{cases} \frac{1}{\Gamma(m-\gamma)} \int_0^t \frac{C^{(m)}(\eta)}{(t-\eta)^{1+\gamma-m}} d\eta, & m-1 < \gamma < m, \\ \frac{d^m}{dt^m} f(t), & \gamma = m \in \mathbb{N} \end{cases} \tag{6}$$

is called time Caputo fractional derivative of order γ $(m-1 < \gamma \leq m)$.

Definition 2. For functions $C(x,t)$ given in the interval $[a,b]$, the expressions [8,16]

$$\frac{\partial^\alpha C(x,t)}{\partial x^\alpha} = \frac{1}{\Gamma(n-\alpha)} \frac{\partial^n}{\partial x^n} \int_a^x \frac{C(\xi,t)d\xi}{(x-\xi)^{\alpha+1-n}}, \quad n = \lceil \alpha \rceil, \tag{7}$$

$$\frac{\partial^\alpha C(x,t)}{\partial (-x)^\alpha} = \frac{(-1)^n}{\Gamma(n-\alpha)} \frac{\partial^n}{\partial x^n} \int_x^b \frac{C(\xi,t)d\xi}{(x-\xi)^{\alpha+1-n}}, \quad n = \lceil \alpha \rceil, \tag{8}$$

are called left- and right-handed Riemann-Liouville derivatives of order α respectively. Here $n = \lceil \alpha \rceil$ is the smallest integer greater than α.

The following five fractional advection-dispersion models as one special case of these models (2):

Model 1: The time FADM with index $0 < \gamma < 1$

If the waiting times of solute particles have infinite mean (where the probability distribution is assumed to decline algebraically with index $0 < \gamma < 1$) and the jump sizes have finite mean and variance, then the scaling limit of such a CTRW has a probability density $C(x,t)$ that evolves according to the following fractional kinetic equation [2,14,23], i.e., $\beta_1 = 0$, $\beta_2 > 0$, $0 < \gamma < 1$, $\alpha = 2$ in the equation (2):

$$\beta_2 \frac{\partial^\gamma C(x,t)}{\partial t^\gamma} = -V \frac{\partial C(x,t)}{\partial x} + D \frac{\partial^2 C(x,t)}{\partial x^2} + f(x,t). \tag{9}$$

The Model 1 was regarded as a subset of the CTRW framework, and it describes solute particles sticking or trapping in relatively immobile domains.

Model 2: The mobile/immobile time FADM $0 < \gamma < 1$

To distinguish explicitly the mobile and immobile status using the fractional dynamics, Schumer et al. [20] developed the following fractional-order, mobile/immobile (MIM) model for the total concentration, i.e., $\beta_1 > 0$, $\beta_2 > 0$,

$0 < \gamma < 1$, $\alpha = 2$ in the equation (2):

$$\beta_1 \frac{\partial C(x,t)}{\partial t} + \beta_2 \frac{\partial^\gamma C(x,t)}{\partial t^\gamma} = -V \frac{\partial C(x,t)}{\partial x} + D \frac{\partial^2 C(x,t)}{\partial x^2} + f(x,t). \tag{10}$$

Model 3: The space FADM with index $1 < \alpha \leq 2$

While sampling heterogeneous soils/aquifers, solute particles can experience various velocity zones. If the complex heterogeneity structure, such as the spatial connectivity, can facilitate movement of particles within a certain scale, fast motions may no longer obey the classical Fickś law and may indeed have a probability density function that follows a power-law. Densities of α-stable type have been used to describe the probability distribution of these motions. The resulting governing equation of these motions is similar to the traditional ADE except that the order α of the highest derivative is fractional. For a large number of independent solute particles the probability propagator is replaced by the expected concentration [8]. A special case of the space FADM may be written as the following form, i.e., $\beta_1 > 0$, $\beta_2 = 0$, $1 < \alpha \leq 2$ in the equation (2):

$$\begin{aligned} \beta_1 \frac{\partial C(x,t)}{\partial t} &= -V \frac{\partial C(x,t)}{\partial x} \\ + D(\frac{1}{2} + \frac{q}{2}) \frac{\partial^\alpha C(x,t)}{\partial x^\alpha} &+ D(\frac{1}{2} - \frac{q}{2}) \frac{\partial^\alpha C(x,t)}{\partial (-x)^\alpha} + f(x,t) \end{aligned} \tag{11}$$

where the parameter $-1 \leq q \leq 1$ called skewness represents the proportion of high-velocity jet in the direction of flow [22,23].

To simulate the anomalously rapid transport of contaminants in heterogeneous systems, we choose $q = 1$, and thus (11) reduces to the following space FADE model with maximally positive skewness:

$$\beta_1 \frac{\partial C(x,t)}{\partial t} = -V \frac{\partial C(x,t)}{\partial x} + D \frac{\partial^\alpha C(x,t)}{\partial x^\alpha} + f(x,t). \tag{12}$$

When $q = -1$, the space FADE (12) reduces to the following space FADE model with maximally negative skewness:

$$\beta_1 \frac{\partial C(x,t)}{\partial t} = -V \frac{\partial C(x,t)}{\partial x} + D \frac{\partial^\alpha C(x,t)}{\partial (-x)^\alpha} + f(x,t). \tag{13}$$

Model 4: The time and space FADM with index $0 < \gamma < 1$ and $1 < \alpha \leq 2$

Field-scale transport studies show that large ranges of solute displacement can be described by a space nonlocal, fractional-derivative model, and long waiting

times can be described efficiently by a time-nonlocal, fractional model. The time and space FADM with index $0 < \gamma < 1$ and $1 < \alpha \leq 2$ may be written as the following form, i.e., $\beta_1 = 0$, $\beta_2 > 0$, $0 < \gamma < 1$, $1 < \alpha \leq 2$ in the equation (2):

$$\beta_2 \frac{\partial^\gamma C(x,t)}{\partial t^\gamma} = -V \frac{\partial C(x,t)}{\partial x} + D(\frac{1}{2} + \frac{q}{2}) \frac{\partial^\alpha C(x,t)}{\partial x^\alpha} + D(\frac{1}{2} - \frac{q}{2}) \frac{\partial^\alpha C(x,t)}{\partial (-x)^\alpha} + f(x,t). \quad (14)$$

Model 5: The time fractional advection-diffusion-wave model with damping with index $1 < \gamma < 2$

The time fractional advection-diffusion-wave model with damping with index $1 < \gamma < 2$, $\alpha = 2$, $\beta_1 > 0$, $\beta_2 > 0$ can be written as the following form:

$$\beta_2 \frac{\partial^\gamma C(x,t)}{\partial t^\gamma} + \beta_1 \frac{\partial C(x,t)}{\partial t} = -V \frac{\partial C(x,t)}{\partial x} + D \frac{\partial^2 C(x,t)}{\partial x^2} + f(x,t). \quad (15)$$

This partial differential equation with $\gamma = 2$ and $V = 0$ is called the telegraph equation which governs electrical transmission in a telegraph cable. It can also be characterized as a fractional diffusion-wave equation (governs wave motion in a string)with a damping effect due to the terms $1 < \gamma < 2$, $V = 0$, $\beta_1 \frac{\partial C(x,t)}{\partial t}$ in the equation (15). Here we can see there is some initial directionality to the wave motion, but this rapidly disappears and the motion becomes completely random. If $1 < \gamma < 2$, $V = 0$, $\beta_1 = 0$, equation (15) reduces to the fractional diffusion-wave equation.

3 Implicit numerical methods for the FADM

In this section, we propose some implicit numerical methods, which can be used to solve the five fractional advection-dispersion models.

Now we construct implicit numerical methods using a new solution technique. We define $t_k = k\tau, k = 0, 1, \ldots, n; x_i = a + ih, i = 0, 1, \ldots, m$, where $\tau = T/n$ and $h = (b-a)/m$ are space and time step sizes, respectively. Assume that $C(x,t) \in C^2([a,b] \times [0,T])$.

Firstly, we consider the case of $0 < \gamma < 1$, i.e., models 1,2,3 and 4.

We discretize the Caputo time fractional derivative using the L1-algorithm

[15,21].

$$\frac{\partial^\gamma C(x,t_{k+1})}{\partial t^\gamma} = \frac{\tau^{-\gamma}}{\Gamma(2-\gamma)} \sum_{j=0}^{k} b_j^\gamma \left[C(x,t_{k+1-j}) - C(x,t_{k-j})\right] + O(\tau^{2-\gamma}), \quad (16)$$

where $b_j^\gamma = (j+1)^{1-\gamma} - j^{1-\gamma},\ j = 0,1,2,\cdots,n.$

Using the relationship between the Grünwald-Letnikov derivative and Riemann-Liouville derivative [16], we discrete the Riemann-Liouville derivatives $\frac{\partial^\alpha C}{\partial x^\alpha}$ and $\frac{\partial^\alpha C}{\partial(-x)^\alpha}$ by the shifted Grünwald-Letnikov formulae [13,16]:

$$\frac{\partial^\alpha}{\partial x^\alpha} C(x_i,t_{k+1}) = \frac{1}{h^\alpha} \sum_{j=0}^{i+1} \omega_j^\alpha C(x_{i+1-j},t_{k+1}) + O(h^p), \quad (17)$$

$$\frac{\partial^\alpha}{\partial(-x)^\alpha} C(x_i,t_{k+1}) = \frac{1}{h^\alpha} \sum_{j=0}^{m-i+1} \omega_j^\alpha C(x_{i-1+j},t_{k+1}) + O(h^p), \quad (18)$$

This formula is not unique because there are many different valid choices for ω_j^α that lead to approximations of different order p [7]. Taking

$$\omega_j^\alpha = (-1)^j \frac{\alpha(\alpha-1)\cdots(\alpha-j+1)}{j!}, \quad j = 0,1,\cdots,$$

then the approximations (17) and (18) provide order $p = 1$.

The first order spatial derivative can be approximated by the backward difference scheme:

$$\frac{\partial C(x_i,t_{k+1})}{\partial x} = \frac{C(x_i,t_{k+1}) - C(x_{i-1},t_{k+1})}{h} + O(h). \quad (19)$$

The first order temporal derivative can be approximated by the backward difference scheme:

$$\frac{\partial C(x_i,t_{k+1})}{\partial t} = \frac{C(x_i,t_{k+1}) - C(x_i,t_k)}{\tau} + O(\tau). \quad (20)$$

Hence, we have

$$
\begin{aligned}
&\beta_1 \frac{C(x_i,t_{k+1})-C(x_i,t_k)}{\tau}+\frac{\beta_2\tau^{-\gamma}}{\Gamma(2-\gamma)}\sum_{j=0}^{k} b_j^{\gamma}\left[C(x,t_{k+1-j})-C(x,t_{k-j})\right]\\
&=-V\frac{C(x_i,t_{k+1})-C(x_{i-1},t_{k+1})}{h}+(\frac{1}{2}+\frac{q}{2})\frac{D}{h^{\alpha}}\sum_{j=0}^{i+1}\omega_j^{\alpha}C(x_{i+1-j},t_{k+1})\\
&+(\frac{1}{2}-\frac{q}{2})\frac{D}{h^{\alpha}}\sum_{j=0}^{m-i+1}\omega_j^{\alpha}C(x_{i-1+j},t_{k+1})+f(x_i,t_{k+1})+R_{i,k+1}. \qquad (21)
\end{aligned}
$$

where

$$
|R_{i,k+1}|\le\begin{cases} A(\tau+h), & \texttt{when}\ \ \beta_1\neq 0,\\ A(\tau^{2-\gamma}+h), & \texttt{when}\ \ \beta_1=0\ \ \texttt{and}\ \ \beta_2\neq 0.\end{cases} \qquad (22)
$$

Let C_i^k be the numerical approximation to $C(x_i,t_k)$ and using Eqs. (16)-(20), then we obtain the following implicit difference approximation of equations (2)-(4):

$$
\begin{aligned}
&\beta_1\frac{C_i^{k+1}-C_i^k}{\tau}+\frac{\beta_2\tau^{-\gamma}}{\Gamma(2-\gamma)}\sum_{j=0}^{k}b_j^{\gamma}\left[C_i^{k+1-j}-C_i^{k-j}\right]\\
&=-V\frac{C_i^{k+1}-C_{i-1}^{k+1}}{h}+(\frac{1}{2}+\frac{q}{2})\frac{D}{h^{\alpha}}\sum_{j=0}^{i+1}\omega_j^{\alpha}C_{i+1-j}^{k+1}\\
&+(\frac{1}{2}-\frac{q}{2})\frac{D}{h^{\alpha}}\sum_{j=0}^{m-i+1}\omega_j^{\alpha}C_{i-1+j}^{k+1}+f(x_i,t_{k+1}) \qquad (23)
\end{aligned}
$$

or

$$
\begin{aligned}
&\mu C_i^{k+1}-r_2C_{i-1}^{k+1}-\tfrac{1+q}{2}r_3\sum_{j=0,j\neq 1}^{i+1}w_j^{\alpha}C_{i+1-j}^{k+1}-\tfrac{1-q}{2}r_3\sum_{j=0,j\neq 1}^{m-i+1}w_j^{\alpha}C_{i-1+j}^{k+1}\\
&=\beta_1C_i^k+\beta_2r_1\left[b_k^{\gamma}C_i^0+\sum_{j=0}^{k-1}(b_j^{\gamma}-b_{j+1}^{\gamma})C_i^{k-j}\right]+\tau f_i^{k+1} \qquad (24)
\end{aligned}
$$

where $r_1=\tau^{1-\gamma}/\Gamma(2-\gamma)$, $r_2=V\tau/h$, $r_3=D\tau/h^{\alpha}$, and $\mu=\beta_1+\beta_2r_1+r_2+\alpha r_3$.

The initial and boundary conditions are discretized as follow

$$
\begin{aligned}
&C_i^0=\varphi(x_i),\quad i=0,1,2,\ldots,m,\\
&C_0^k=\phi_1(k\tau),\quad C_m^k=\phi_2(k\tau),\quad k=1,2,\ldots,n. \qquad (25)
\end{aligned}
$$

Lemma 1. The coefficients b_j^{γ}, $w_j^{\alpha}, j=0,1,2,\cdots$, satisfy:

$(1) b_0^{\gamma}=1,\quad b_j^{\gamma}>0,\quad j=1,2,\cdots;$

(2)$b_j^\gamma > b_{j+1}^\gamma, \quad j = 0, 1, \cdots;$

(3)$w_0^\alpha = 1, \quad w_1^\alpha = -\alpha < 0, \quad$ and $w_j^\alpha > 0, j = 2, 3, \cdots;$

(4)$\sum\limits_{j=0}^{\infty} w_j^\alpha = 0, \quad$ and for $i = 1, 2, \cdots$, we have $\quad \sum\limits_{j=0}^{i} w_j^\alpha < 0.$

Proof. See [9].

From $\lim\limits_{k\to\infty} \frac{(b_k^\gamma)^{-1}}{k^\gamma} = \lim\limits_{k\to\infty} \frac{k^{-1}}{(1+\frac{1}{k})^{1-\gamma}-1} = \frac{1}{1-\gamma}$, we obtain the following lemma.

Remark 1 From Lemma 1, we see that the coefficient matrix A of the systems (24) is strictly diagonally dominant with positive diagonal terms and nonpositive off-diagonal terms. Hence, the discretization matrix A is invertible. Furthermore, the system (24) and (25) has a unique solution.

Lemma 2. If $0 < \gamma < 1$, there is a positive constant ρ such that

$$(b_k^\gamma)^{-1} \le \rho k^\gamma, k = 1, 2, \cdots \tag{26}$$

Now we consider the case of $1 < \gamma = \bar{\gamma} + 1 < 2$, i.e., Model 5.

Let $U(x,t) = \frac{\partial C(x,t)}{\partial t}$, the equation (15) can be rewritten as

$$\begin{cases} \frac{\partial C}{\partial t} = U \\ \beta_2 \frac{\partial^{\bar{\gamma}} U}{\partial t^{\bar{\gamma}}} + \beta_1 U = -V \frac{\partial C(x,t)}{\partial x} + D \frac{\partial^2 C(x,t)}{\partial x^2} + f(x,t) \end{cases} \tag{27}$$

where $0 < \bar{\gamma} < 1$. Hence, we can obtain the following difference scheme

$$\begin{cases} \quad \frac{\Delta_t C_i^k}{\tau} = U_i^{k+1}, \\ \quad \beta_2 \frac{\tau^{-\bar{\gamma}}}{\Gamma(2-\bar{\gamma})} \sum\limits_{j=0}^{k} b_j^{\bar{\gamma}} \Delta_t U_i^{k-j} + \beta_1 U_i^{k+1} \\ = -V \frac{C_i^{k+1} - C_{i-1}^{k+1}}{h} + D \frac{C_{i-1}^{k+1} - 2C_i^{k+1} + C_{i-1}^{k+1}}{h^2} + f_i^{k+1}, \end{cases} \tag{28}$$

where $\Delta_t C_i^k = C_i^{k+1} - C_i^k$ and $f_i^{k+1} = f(x_i, t_{k+1})$. Thus, the above second equation can be rewritten as

$$\begin{aligned} &(\beta_2 + \beta_1\bar{\mu} + \bar{r}_1 + 2\bar{r}_2)C_i^{k+1} - (\bar{r}_1 + \bar{r}_2)C_{i-1}^{k+1} - \bar{r}_2 C_{i+1}^{k+1} \\ &= (\beta_2 + \beta_1\bar{\mu})C_i^k + \tau \left[b_k^{\bar{\gamma}} U_i^0 + \sum_{j=0}^{k-1} (b_j^{\bar{\gamma}} - b_{j+1}^{\bar{\gamma}}) U_i^{k-j} \right] + \bar{\mu}\tau f_i^{k+1}, \end{aligned} \tag{29}$$

where $\bar{\mu} = \tau^{\bar{\gamma}}\Gamma(2-\bar{\gamma})$, $\bar{r}_1 = V\bar{\mu}\tau/h$, $\bar{r}_2 = D\bar{\mu}\tau/h^2$.

Remark 2 The coefficient matrix of the systems (29) is strictly diagonally dominant with positive diagonal terms and nonpositive off-diagonal terms. Hence, the system (28) is solvable.

4 Stability of the implicit numerical methods for the FADM

In this section, we discuss the implicit numerical methods (24) with boundary conditions $C_0^k = C_m^k = 0, k = 0, 1, 2, \ldots, n$.

Definition 3. A finite difference scheme is said to be stable for the norm $\|\cdot\|$, if there exists two constants $\lambda_1 > 0$ and $\lambda_2 > 0$, independent of h and τ, such that when h and τ tend towards zero:

$$\|C^k\| \leq \lambda_1 \|C^0\| + \lambda_2 \|f\|, \quad \forall k > 0,$$

whatever the initial data C^0 and the source term f.

Let $\|\mathbf{C}^{k+1}\|_\infty = \max\limits_{1\leq i\leq m-1} |C_i^{k+1}|$ and $\|\mathbf{f}\|_\infty = \max\limits_{0\leq i\leq m; 0\leq k\leq n} |f_i^k|$.

Lemma 3. Assume that $C_i^k (i = 1, 2, \cdots, m-1; k = 1, 2, \cdots, n)$ be the numerical solution of (24). If $|C_{i_0}^{k+1}| = \max\limits_{1\leq i\leq m-1} |C_i^{k+1}|$, then

$$\begin{aligned}
&(\beta_1 + \beta_2 r_1)\|\mathbf{C}^{k+1}\|_\infty \\
&\leq |\beta_1 C_{i_0}^k + \beta_2 r_1 [b_k^\gamma C_{i_0}^0 + \sum_{j=0}^{k-1} (b_j^\gamma - b_{j+1}^\gamma) C_{i_0}^{k-j}] + \tau f_{i_0}^{k+1}|
\end{aligned}$$

Proof. Using $\sum\limits_{l=0}^{i_0+1} w_l^\alpha < 0$, $\sum\limits_{l=0}^{m-i_0+1} w_l^\alpha < 0$, we have

$$\begin{aligned}
&(\beta_1 + \beta_2 r_1)\|\mathbf{C}^{k+1}\|_\infty \\
&= |(\beta_1 + \beta_2 r_1) C_{i_0}^{k+1}| \\
&\leq (\mu - r_2 - \tfrac{1+q}{2} r_3 \sum_{j=0, j\neq 1}^{i+1} w_j^\alpha - \tfrac{1-q}{2} r_3 \sum_{j=0, j\neq 1}^{m-i+1} w_j^\alpha) |C_{i_0}^{k+1}| \\
&\leq \mu |C_{i_0}^{k+1}| - r_2 |C_{i_0-1}^{k+1}| - \tfrac{1+q}{2} r_3 \sum_{j=0, j\neq 1}^{i+1} w_j^\alpha |C_{i_0+1-j}^{k+1}| - \tfrac{1-q}{2} r_3 \sum_{j=0, j\neq 1}^{m-i+1} w_j^\alpha |C_{i_0-1+j}^{k+1}| \\
&\leq |\mu C_{i_0}^{k+1} - r_2 C_{i_0-1}^{k+1} - \tfrac{1+q}{2} r_3 \sum_{j=0, j\neq 1}^{i+1} w_j^\alpha C_{i_0+1-j}^{k+1} - \tfrac{1-q}{2} r_3 \sum_{j=0, j\neq 1}^{m-i+1} w_j^\alpha C_{i_0-1+j}^{k+1}| \\
&= |\beta_1 C_{i_0}^k + \beta_2 r_1 [b_k^\gamma C_{i_0}^0 + \sum_{j=0}^{k-1} (b_j^\gamma - b_{j+1}^\gamma) C_{i_0}^{k-j}] + \tau f_{i_0}^{k+1}|.
\end{aligned}$$

Therefore, the conclusion of the Lemma 3 is proved.

Theorem 1. Assume that $C_i^k (i = 1, 2, \cdots, m-1; k = 1, 2, \cdots, n)$ be the numerical solution of (24). If $\beta_1 \neq 0$, then

$$(\beta_1 + \beta_2 r_1) \max_{1 \le j \le k} \|\mathbf{C}^j\|_\infty \le (\beta_1 + \beta_2 r_1) \|\mathbf{C}^0\|_\infty + k\tau \|\mathbf{f}\|_\infty. \tag{30}$$

Further, we have

$$\|\mathbf{C}^k\|_\infty \le \|\mathbf{C}^0\|_\infty + \frac{k\tau}{\beta_1} \|\mathbf{f}\|_\infty, \quad k = 1, 2, \cdots, n. \tag{31}$$

Proof. Let $|C_{i_0}^{k+1}| = \max\limits_{1 \le i \le m-1} |C_i^{k+1}|$. By Lemma 3, we obtain

$$\begin{aligned}
&|(\beta_1 + \beta_2 r_1) C_{i_0}^{k+1}| \\
&\le |\beta_1 C_{i_0}^k + \beta_2 r_1 [b_k^\gamma C_{i_0}^0 + \sum_{j=0}^{k-1} (b_j^\gamma - b_{j+1}^\gamma) C_{i_0}^{k-j}] + \tau f_{i_0}^{k+1}| \\
&\le \left\{ \beta_1 + \beta_2 r_1 [b_k^\gamma + \sum_{j=0}^{k-1} (b_j^\gamma - b_{j+1}^\gamma)] \right\} \max_{1 \le j \le k} \|\mathbf{C}^j\|_\infty + \tau \|\mathbf{f}\|_\infty \\
&= \{\beta_1 + \beta_2 r_1\} \max_{1 \le j \le k} \|\mathbf{C}^j\|_\infty + \tau \|\mathbf{f}\|_\infty
\end{aligned}$$

i.e.,

$$(\beta_1 + \beta_2 r_1) \max_{1 \le j \le k+1} \|\mathbf{C}^j\|_\infty \le (\beta_1 + \beta_2 r_1) \max_{1 \le j \le k} \|\mathbf{C}^j\|_\infty + \tau \|\mathbf{f}\|_\infty.$$

Thus,

$$(\beta_1 + \beta_2 r_1) \max_{1 \le j \le k+1} \|\mathbf{C}^j\|_\infty \le (\beta_1 + \beta_2 r_1) \|\mathbf{C}^0\|_\infty + (k+1)\tau \|\mathbf{f}\|_\infty. \tag{32}$$

Therefore, the conclusion of the theorem is proved.

Theorem 2. Assume that $C_i^k (i = 1, 2, \cdots, m-1; k = 1, 2, \cdots, n)$ be the numerical solution of (24). If $\beta_1 = 0$ and $\beta_2 \neq 0$, then

$$\|\mathbf{C}^j\|_\infty \le \|\mathbf{C}^0\|_\infty + (b_{j-1}^\gamma \beta_2 r_1)^{-1} \tau \|\mathbf{f}\|_\infty, \quad j = 1, 2, \ldots, n. \tag{33}$$

Further,

$$\|\mathbf{C}^j\|_\infty \le \|\mathbf{C}^0\|_\infty + \lambda (j\tau)^\gamma \|\mathbf{f}\|_\infty, \quad j = 1, 2, \ldots, n, \tag{34}$$

where λ is a positive constant.

Proof. For $j = 1$, we assume that $|C_{i_0}^1| = \max\limits_{1 \le i \le m-1} |C_i^1|$. Applying Lemma 3, we have

$$|\beta_2 r_1 C_{i_0}^1| \le |\beta_2 r_1 b_0^\gamma C_{i_0}^0 + \tau f_{i_0}^1|.$$

Thus, $\beta_2 r_1 \|\mathbf{C}^1\|_\infty \le \beta_2 r_1 \|\mathbf{C}^0\|_\infty + \tau \|\mathbf{f}\|_\infty$, i. e.,

$$\|\mathbf{C}^1\|_\infty \le \|\mathbf{C}^0\|_\infty + (b_0^\gamma \beta_2 r_1)^{-1} \tau \|\mathbf{f}\|_\infty.$$

Suppose that

$$\|\mathbf{C}^j\|_\infty \le \|\mathbf{C}^0\|_\infty + (b_{j-1}^\gamma \beta_2 r_1)^{-1}\tau\|\mathbf{f}\|_\infty, \quad 1 \le j \le k. \tag{35}$$

When $j = k+1$, we assume that $|C_{i_0}^{k+1}| = \max\limits_{1\le i\le m-1} |C_i^{k+1}|$. By Lemma 3, we obtain

$$|\beta_2 r_1 C_{i_0}^{k+1}| \le |\beta_2 r_1 [b_k^\gamma C_{i_0}^0 + \sum_{j=0}^{k-1}(b_j^\gamma - b_{j+1}^\gamma) C_{i_0}^{k-j}] + \tau f_{i_0}^{k+1}|.$$

Therefore,

$$\beta_2 r_1 \|C^{k+1}\|_\infty \le \beta_2 r_1 [b_k^\gamma \|C^0\|_\infty + \sum_{j=0}^{k-1}(b_j^\gamma - b_{j+1}^\gamma)\|C^{k-j}\|_\infty] + \tau\|\mathbf{f}\|_\infty.$$

Using the induction hypothesis (35) and $(b_j^\gamma)^{-1} < (b_k^\gamma)^{-1} (0 \le j \le k-1)$, we obtain

$$\|\mathbf{C}^j\|_\infty \le \|\mathbf{C}^0\|_\infty + (b_k^\gamma \beta_2 r_1)^{-1}\tau\|\mathbf{f}\|_\infty, \quad 1 \le j \le k.$$

Thus, we have

$$\begin{aligned}\beta_2 r_1 \|C^{k+1}\|_\infty \le\ & \beta_2 r_1 [b_k^\gamma + \sum_{j=0}^{k-1}(b_j^\gamma - b_{j+1}^\gamma)]\|C^0\|_\infty \\ & + \beta_2 r_1 \sum_{j=0}^{k-1}(b_j^\gamma - b_{j+1}^\gamma)(b_k^\gamma \beta_2 r_1)^{-1}\tau\|\mathbf{f}\|_\infty + \tau\|\mathbf{f}\|_\infty.\end{aligned}$$

Further, we obtain

$$\begin{aligned}\|C^{k+1}\|_\infty \le\ & \left\{[b_k^\gamma + \sum_{j=0}^{k-1}(b_j^\gamma - b_{j+1}^\gamma)]\right\}\|C^0\|_\infty \\ & + \sum_{j=0}^{k-1}(b_j^\gamma - b_{j+1}^\gamma)(b_k^\gamma \beta_2 r_1)^{-1}\tau\|\mathbf{f}\|_\infty + (\beta_2 r_1)^{-1}\tau\|\mathbf{f}\|_\infty.\end{aligned}$$

i. e.,

$$\begin{aligned}\|\mathbf{C}^{k+1}\|_\infty &\le \|\mathbf{C}^0\|_\infty + [b_k^\gamma + \sum_{j=0}^{k-1}(b_j^\gamma - b_{j+1}^\gamma)](b_k^\gamma \beta_2 r_1)^{-1}\tau\|\mathbf{f}\|_\infty \\ &= \|\mathbf{C}^0\|_\infty + (b_k^\gamma \beta_2 r_1)^{-1}\tau\|\mathbf{f}\|_\infty.\end{aligned}$$

Therefore,

$$\|\mathbf{C}^j\|_\infty \le \|\mathbf{C}^0\|_\infty + (b_{j-1}^\gamma \beta_2 r_1)^{-1}\tau\|\mathbf{f}\|_\infty, \quad j = 1, 2, \ldots, n.$$

By Lemma 2, we can obtain

$$\|\mathbf{C}^j\|_\infty \le \|\mathbf{C}^0\|_\infty + \lambda(j\tau)^\gamma\|\mathbf{f}\|_\infty, \quad j = 1, 2, \ldots, n,$$

where $\lambda = \rho(\beta_2)^{-1}\Gamma(2-\gamma)$.

Hence, the conclusion of the theorem is proved.

Let $\widetilde{C}_i^k, (0 \le i \le m; 0 \le j \le n)$ be the approximate solution of (24), the error $\varepsilon_i^k = \widetilde{C}_i^k - C_i^k, (0 \le i \le m; 0 \le k \le n)$ satisfies

$$\begin{aligned} &\mu\varepsilon_i^{k+1} - r_2\varepsilon_{i-1}^{k+1} - \tfrac{1+q}{2}r_3 \sum_{j=0,j\neq 1}^{i+1} w_j^\alpha \varepsilon_{i+1-j}^{k+1} - \tfrac{1-q}{2}r_3 \sum_{j=0,j\neq 1}^{m-i+1} w_j^\alpha \varepsilon_{i-1+j}^{k+1} \\ &= \beta_1\varepsilon_i^k + \beta_2 r_1 \left[b_k^\gamma \varepsilon_i^0 + \sum_{j=0}^{k-1} (b_j^\gamma - b_{j+1}^\gamma)\varepsilon_i^{k-j} \right]. \end{aligned} \tag{36}$$

Applying Theorem 1 and Theorem 2, we can obtain

$$\|\mathbf{E}^k\|_\infty \le \|\mathbf{E}^0\|_\infty, \quad k = 1, 2, \cdots, n,$$

where $\|\mathbf{E}^k\|_\infty = \max\limits_{1\le i\le m-1} |\varepsilon_i^k|$. The following conclusion is obtained.

Theorem 3. The fractional implicit numerical method defined by (24) is unconditionally stable.

Remark 1: Using similar method, we can investigate the stability of the fractional implicit numerical method defined by (28).

5 Convergence of the implicit numerical methods

Now we investigate the convergence of the implicit numerical methods (23).

Let $C(x_i, t_k), (i = 1, 2, \ldots, m-1; k = 1, 2, \ldots, n)$ be the exact solution of the equations (2)-(4) at mesh point (x_i, t_k). Define $\eta_i^k = C(x_i, t_k) - C_i^k, i = 1, 2, \ldots, m-1; k = 1, 2, \ldots, n$ and $\mathbf{Y}^k = (\eta_1^k, \eta_2^k, \cdots, \eta_{m-1}^k)^T$. From (21) and (23), we obtain

$$\begin{aligned} &\mu\eta_i^{k+1} - r_2\eta_{i-1}^{k+1} - \tfrac{1+q}{2}r_3 \sum_{j=0,j\neq 1}^{i+1} w_j^\alpha \eta_{i+1-j}^{k+1} - \tfrac{1-q}{2}r_3 \sum_{j=0,j\neq 1}^{m-i+1} w_j^\alpha \varepsilon_{i-1+j}^{k+1} \\ &= \beta_1\eta_i^k + \beta_2 r_1 \left[b_k^\gamma \eta_i^0 + \sum_{j=0}^{k-1} (b_j^\gamma - b_{j+1}^\gamma)\eta_i^{k-j} \right] + \tau R(x_i, t_k), \end{aligned} \tag{37}$$

where $i = 1, 2, \cdots, m-1, k = 0, 1, 2, \cdots, n-1$.

Applying Theorem 1 and Theorem 2, by (22), we obtain the following convergence theorem.

Theorem 4. Let C_i^k be the numerical solution computed by use of the implicit numerical methods (24) and (25), $C(x, t)$ is the solution of the problem (2)-(4).

Then there is a positive constant A , such that

$$|C_i^k - C(x_i, t_k)| \leq \begin{cases} A(\tau + h), & \texttt{when} \ \ \beta_1 \neq 0, \\ A(\tau^{2-\gamma} + h), & \texttt{when} \ \ \beta_1 = 0 \ \ \texttt{and} \ \ \beta_2 \neq 0, \end{cases} \tag{38}$$

where $i = 1, 2, \cdots, m-1; k = 1, 2, \ldots, n$.

Remark 2: Using similar method, we can investigate the convergence of the fractional implicit numerical method defined by (28) or (29).

6 Numerical results

In order to demonstrate the effectiveness of our theoretical analysis, some examples are now presented. These implicit numerical methods can be used to simulate regional-scale anomalous dispersion with heavy tails.

Example 1: Consider the following space-time fractional advection-diffusion equation

$$\begin{aligned} \tfrac{\partial C(x,t)}{\partial t} + \tfrac{\partial^\gamma C(x,t)}{\partial t^\gamma} = -\tfrac{\partial C(x,t)}{\partial x} + \tfrac{1}{2}\left[\tfrac{\partial^\alpha C(x,t)}{\partial x^\alpha} + \tfrac{\partial^\alpha C(x,t)}{\partial (-x)^\alpha}\right] + f(x,t), \\ (x,t) \in [0,1] \times [0,T] \end{aligned} \tag{39}$$

together with the following boundary and initial conditions

$$\begin{cases} C(0,t) = C(1,t) = 0, & 0 \leq t \leq T, \\ C(x,0) = 0, & 0 \leq x \leq 1 \end{cases} \tag{40}$$

where $\gamma = 0.85$, $\alpha = 1.80$, $f(x,t) = f_1(x,t) + f_2(x,t) - f_3(x,t) - f_4(x,t)$, and

$$\begin{aligned} f_1(x,t) &= 2(t + \tfrac{t^{2-\gamma}}{3-\gamma})x^2(1-x)^2, \\ f_2(x,t) &= 2x(1-x)(1-2x)t^2, \\ f_3(x,t) &= \tfrac{2x^{2-\alpha}t^2}{\Gamma(5-\alpha)}\left[(3-\alpha)(4-\alpha) - 6(4-\alpha)x + 12x^2\right], \\ f_4(x,t) &= \tfrac{2(1-x)^{2-\alpha}t^2}{\Gamma(5-\alpha)}\left[(3-\alpha)(4-\alpha) - 6(4-\alpha)(1-x) + 12(1-x)^2\right]. \end{aligned}$$

The exact solution to this problem can be easily obtained as $u(x,t) = t^2x^2(1-x)^2$.

Figs. 1 and 2 show the exact and numerical solutions with $\alpha = 1.8$ and $\gamma = 0.85$ at $T = 1$ and $x = 0.4$, respectively. From Figs. 1 and 2, it can be seen that the implicit numerical methods are in excellent agreement with the exact solution.

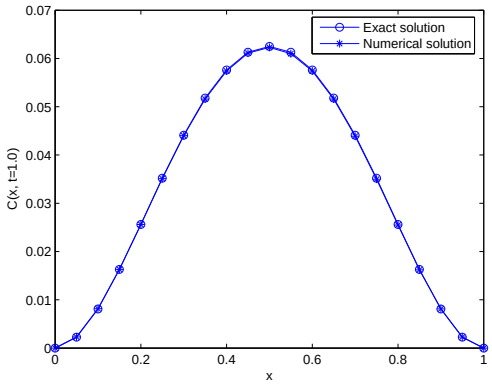

Fig. 1. Comparison between the exact solution and the numerical solution when $T = 1$ with $\alpha = 1.8$ and $\gamma = 0.85$ in Example 1.

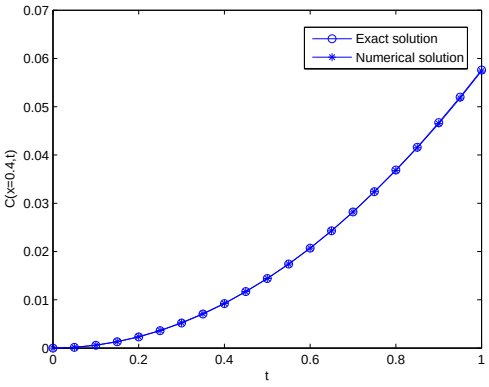

Fig. 2. Comparison between the exact solution and the numerical solution at $x = 0.4$ with $\alpha = 1.8$ and $\gamma = 0.85$ in Example 1.

Taking $\beta_1 = \beta_2 = 1$, Fig. 1 shows the exact and numerical solutions with $\alpha = 1.8$ and $\gamma = 0.85$ at $T = 1$. From Fig. 1, it can be seen that the implicit numerical methods are in excellent agreement with the exact solution.

Let

$$\|E\|_{\max} = \max_{1\le i\le m-1} |C(x_i, t_n) - C_i^n|. \tag{41}$$

From Table 1 and Table 2, we can conclude that

$$\|E\|_{\max} \le C_1(\tau + h), \quad \texttt{when}\beta_1 = \beta_2 = 1 \tag{42}$$

and

$$\|E\|_{\max} \le C_2(\tau^{2-\gamma} + h), \quad \texttt{when}\beta_1 = 0, \quad \beta_2 = 1. \tag{43}$$

where $C_1 = 0.012$ and $C_2 = 0.0126$.

Table 1
The numerical errors using the implicit difference approximation (24) for $\beta_1 = \beta_2 = 1$ at $t = 1.0$

τ	h	Maximum Error $\|E\|_{\max}$
5.0e-2	5.0e-2	8.4480e-4
2.5e-2	2.5e-2	5.0475e-4
1.25e-2	1.25e-2	2.7483e-4
6.25e-3	6.25e-3	1.4388e-4

Example 2: Consider the following variable coefficient space-time fractional

Table 2
The numerical errors using the implicit difference approximation (24) for $\beta_1 = 0$ and $\beta_2 = 1$ at $t = 1.0$

τ	$h = \tau^{2-\gamma}$	Maximum Error $\|E\|_{\max}$
5.0e-2	3.190e-2	1.0055e-3
2.5e-2	1.438e-2	4.9461e-4
1.25e-2	6.478e-3	2.2581e-4
6.25e-3	2.919e-3	1.0407 e-4

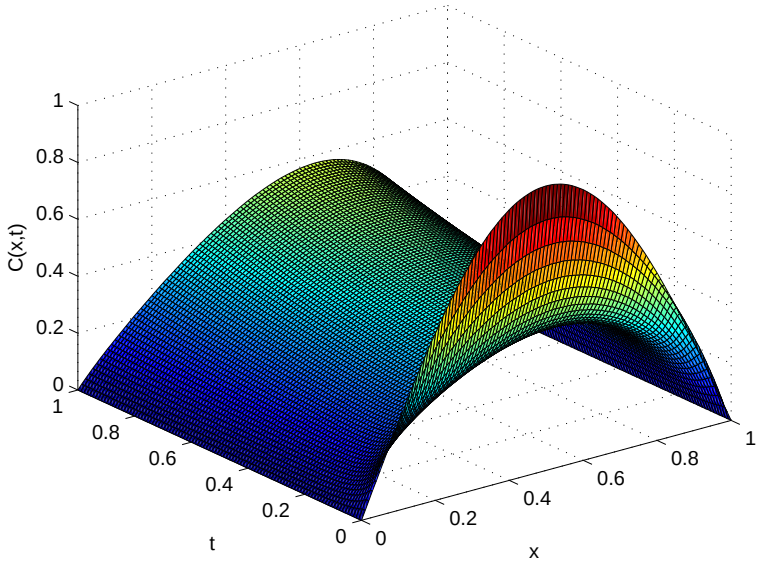

Fig. 3. The approximation solution of (44)-(45) when $\alpha = 1.8$ and $\gamma = 0.85$ in Example 2.

advection-diffusion equation

$$\frac{\partial C(x,t)}{\partial t} + \frac{\partial^\gamma C(x,t)}{\partial t^\gamma} = -(1+x^2t^2)\frac{\partial C(x,t)}{\partial x} + (1+x+t)\left[\frac{\partial^\alpha C(x,t)}{\partial x^\alpha} + \frac{\partial^\alpha C(x,t)}{\partial(-x)^\alpha}\right] + e^{xt}, \quad (x,t) \in [0,1]\times[0,1] \tag{44}$$

together with the following boundary and initial conditions

$$\begin{cases} C(0,t) = C(1,t) = 0, & 0 \le t \le 1, \\ C(x,0) = \sin x, & 0 \le x \le 1 \end{cases} \tag{45}$$

where $\gamma = 0.85$, $\alpha = 1.80$. The exact solution is not available.

Fig. 3 shows the numerical solutions with $\alpha = 1.8, \quad \gamma = 0.85$.

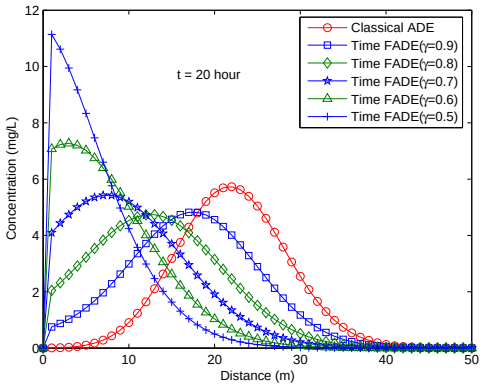

Fig. 4. The numerical approximation whose transport is governed by the time FADE (48) for various $\gamma = 1, 0.9, 0.8, 0.7, 0.6, 0.5$ when $T = 20$.

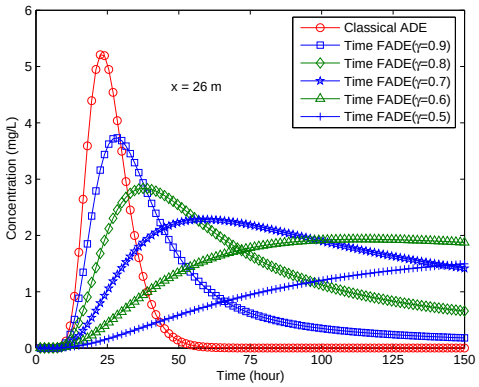

Fig. 5. The numerical approximation whose transport is governed by the time FADE (48) for various $\gamma = 1, 0.9, 0.8, 0.7, 0.6, 0.5$ when $x = 26$.

In the following numerical examples, we consider the time, space and space-time fractional advection-diffusion models with instantaneous source for the $0 < \gamma < 1$ case, i.e., models 1, 2, 3 and 4.

$$\beta_1 \frac{\partial C}{\partial t} + \beta_2 \frac{\partial^\gamma C}{\partial t^\gamma} = -V \frac{\partial C}{\partial x} + D(\frac{1}{2} + \frac{q}{2}) \frac{\partial^\alpha C}{\partial x^\alpha} + D(\frac{1}{2} - \frac{q}{2}) \frac{\partial^\alpha C}{\partial (-x)^\alpha} + c_0 x_0 \delta(x, t), \tag{46}$$

with the boundary conditions

$$C(0, t) = 0, \quad \frac{\partial C(b, t)}{\partial x} = 0, \quad 0 < t \leq T, \tag{47}$$

where $c_0 x_0 \delta(x, t)$ denotes the initial solute concentration, c_0 being the spread over some injection distance x_0 which is mathematically concentrated into a delta function, $c_0 = 1000$.

Example 3 (Model 1): Consider the following the time FADM with $0 < \gamma < 1$:

$$\frac{\partial^\gamma C(x, t)}{\partial t^\gamma} = -\frac{\partial C(x, t)}{\partial x} + \frac{\partial^2 C(x, t)}{\partial x^2} + c_0 x_0 \delta(x, t). \tag{48}$$

The computational results for different γ at $T = 20$ and $x = 26$ are shown in Figs. 4 and 5, respectively. Figs. 4 and 5 show that the order of the fractional time derivative γ governs the probability tails of the delay between jumps. The model 1 describes solute particles sticking or trapping in relatively immobile domains.

Example 4 (Model 2):

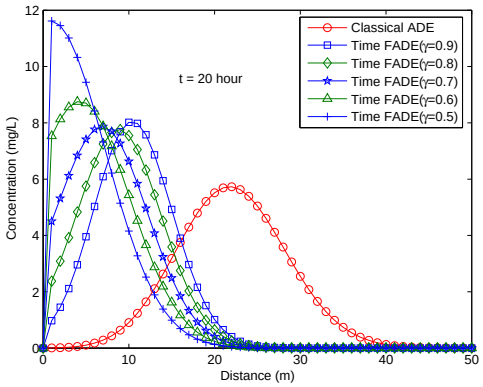

Fig. 6. The numerical approximation whose transport is governed by the time FADE (49) for various $\gamma = 1, 0.9, 0.8, 0.7, 0.6, 0.5$ when $T = 20$.

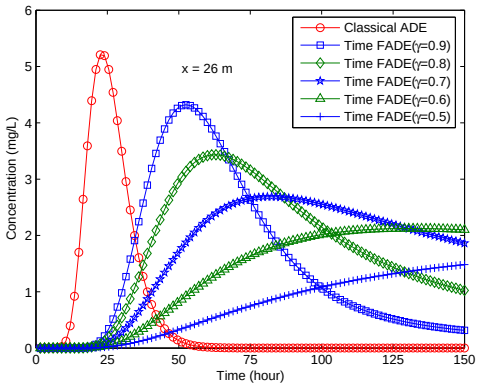

Fig. 7. The numerical approximation whose transport is governed by the time FADE (49) for various $\gamma = 1, 0.9, 0.8, 0.7, 0.6, 0.5$ when $x = 26$.

Consider the following The mobile/immobile time FADE with $0 < \gamma < 1$:

$$\frac{\partial C(x,t)}{\partial t} + \frac{\partial^\gamma C(x,t)}{\partial t^\gamma} = -\frac{\partial C(x,t)}{\partial x} + \frac{\partial^2 C(x,t)}{\partial x^2} + c_0 x_0 \delta(x,t). \qquad (49)$$

The model provides the mobile/immobile CTRW models by dividing the transition time into mobile and immobile parts. The computational results for different γ at $T = 20$ and $x = 26$ are shown in Figs. 6 and 7, respectively. Figures 6 and 7 show that the time drift term $\frac{\partial C(x,t)}{\partial t}$ is added to described the motion time and thus help to distinguish the status of particles conveniently [23]. The corresponding fractional-derivative governing equations for the mobile and immobile phases can be found in [20].

Example 5 (Model 3):

Consider the following space FADE with $1 < \alpha \leq 2$:

$$\frac{\partial C(x,t)}{\partial t} = -\frac{\partial C(x,t)}{\partial x} + (\frac{1}{2} + \frac{q}{2})\frac{\partial^\alpha C(x,t)}{\partial x^\alpha} + (\frac{1}{2} - \frac{q}{2})\frac{\partial^\alpha C(x,t)}{\partial (-x)^\alpha} + c_0 x_0 \delta(x,t), \qquad (50)$$

where the parameter $-1 \leq q \leq 1$ called skewness represents the proportion of high-velocity jet in the direction of flow [8,23]. The parameter q describes the "skewness" of the transport process. Numerical approximation of the space FADM with index $1 < \alpha \leq 2$ is used to simulate Lévy motion with $\alpha-$stable densities.

When $q = 1$, and thus (50) reduces to the following space FADM with maxi-

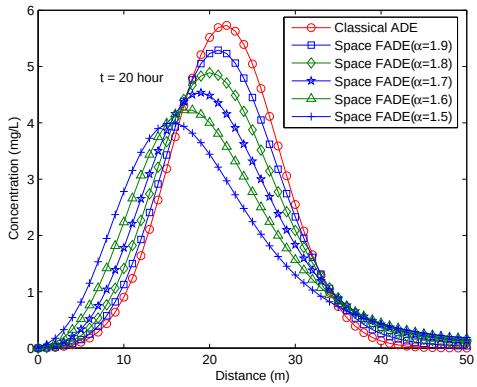

Fig. 8. The numerical approximation whose transport is governed by the space FADE (51) for various $\alpha = 2, 1.9, 1.8, 1.7, 1.6, 1.5$ when $T = 20$.

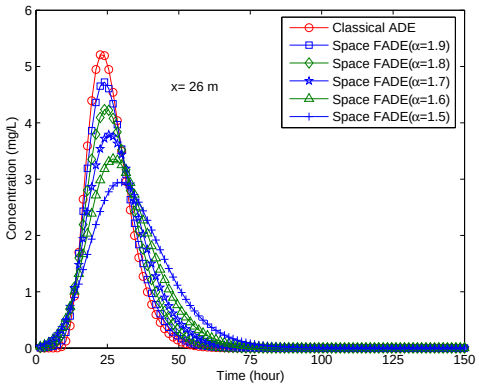

Fig. 9. The numerical approximation whose transport is governed by the space FADE (51) for various $\alpha = 2, 1.9, 1.8, 1.7, 1.6, 1.5$ when $x = 26$.

mally positive skewness:

$$\frac{\partial C(x,t)}{\partial t} = -\frac{\partial C(x,t)}{\partial x} + \frac{\partial^\alpha C(x,t)}{\partial x^\alpha} + c_0 x_0 \delta(x,t). \tag{51}$$

The computational results for different α at $T = 20$ and $x = 26$ are shown in Figs. 8 and 9, respectively.

When $q = -1$, the space FADE (50) reduces to the following space FADM with maximally negative skewness:

$$\frac{\partial C(x,t)}{\partial t} = -\frac{\partial C(x,t)}{\partial x} + \frac{\partial^\alpha C(x,t)}{\partial (-x)^\alpha} + c_0 x_0 \delta(x,t). \tag{52}$$

The computational results for different α at $T = 20$ and $x = 26$ are shown in Figures 10 and 11, respectively.

When $q = 0$, the space FADM (50) reduces to a symmetric transition processes.

$$\frac{\partial C(x,t)}{\partial t} = -\frac{\partial C(x,t)}{\partial x} + \frac{1}{2}\frac{\partial^\alpha C(x,t)}{\partial x^\alpha} + \frac{1}{2}\frac{\partial^\alpha C(x,t)}{\partial (-x)^\alpha} + c_0 x_0 \delta(x,t). \tag{53}$$

The computational results for different α at $T = 20$ and $x = 26$ are shown in Figs. 12 and 13, respectively.

Example 6 (Model 4):

Consider the following space-time fractional differential equation with $0 < \gamma < 1$ and $1 < \alpha \leq 2$:

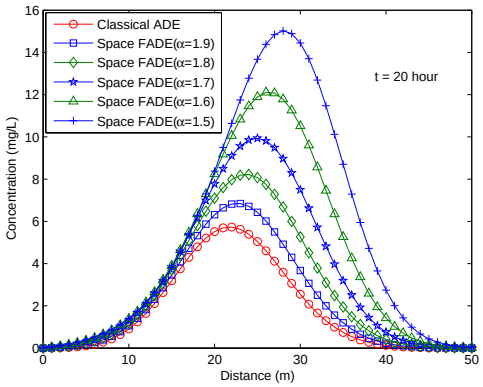

Fig. 10. The numerical approximation whose transport is governed by the space FADE (52) for various $\alpha = 2, 1.9, 1.8, 1.7, 1.6, 1.5$ when $T = 20$.

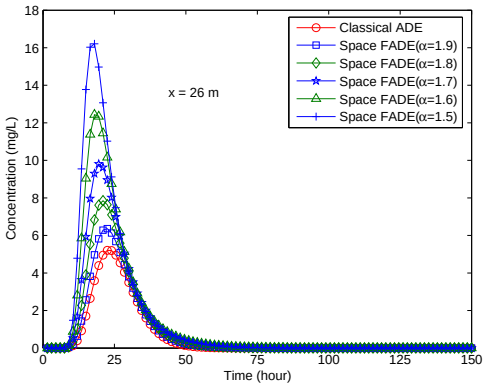

Fig. 11. The numerical approximation whose transport is governed by the space FADE (52) for various $\alpha = 2, 1.9, 1.8, 1.7, 1.6, 1.5$ when $x = 26$.

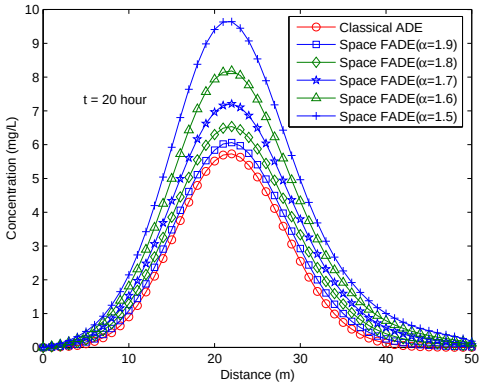

Fig. 12. The numerical approximation whose transport is governed by the space FADE (53) for various $\alpha = 2, 1.9, 1.8, 1.7, 1.6, 1.5$ when $T = 20$.

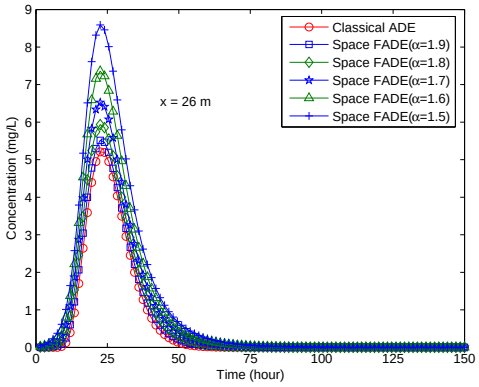

Fig. 13. The numerical approximation whose transport is governed by the space FADE (53) for various $\alpha = 2, 1.9, 1.8, 1.7, 1.6, 1.5$ when $x = 26$.

$$\frac{\partial^\gamma C(x,t)}{\partial t^\gamma} = -\frac{\partial C(x,t)}{\partial x} + (\frac{1}{2}+\frac{q}{2})\frac{\partial^\alpha C(x,t)}{\partial x^\alpha} + D(\frac{1}{2}-\frac{q}{2})\frac{\partial^\alpha C(x,t)}{\partial(-x)^\alpha} + f(x,t). \quad (54)$$

The computational results for different γ at $T = 20$ and $x = 26$ are shown in Figs. 14-17, respectively.

Example 7 (Model 5):

Consider the following advection-diffusion-wave model with damping with $1 <$

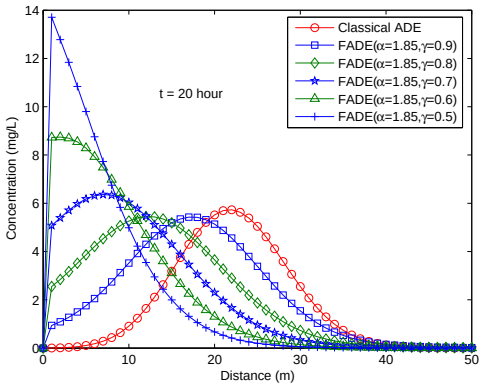

Fig. 14. The numerical approximation whose transport is governed by the space and time FADE (54) for $\alpha = 1.85$ and various $\gamma = 1, 0.9, 0.8, 0.7, 0.6, 0.5$ when $T = 20$.

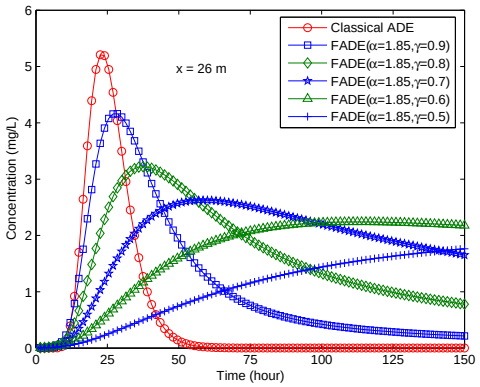

Fig. 15. The numerical approximation whose transport is governed by the space and time FADE (54) for $\alpha = 1.85$ and various $\gamma = 1, 0.9, 0.8, 0.7, 0.6, 0.5$ when $x = 26$.

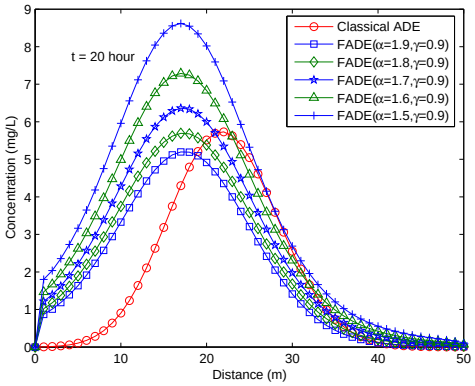

Fig. 16. The numerical approximation whose transport is governed by the space and time FADE (54) for $\gamma = 0.9$ and various $\alpha = 2, 1.9, 1.8, 1.7, 1.6, 1.5$ when $T = 20$.

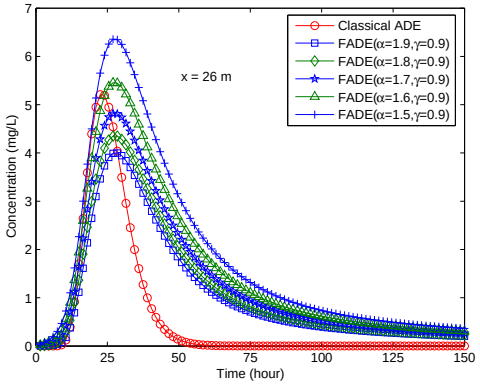

Fig. 17. The numerical approximation whose transport is governed by the space and time FADE (54) for $\gamma = 0.9$ and various $\alpha = 2, 1.9, 1.8, 1.7, 1.6, 1.5$ when $x = 26$.

$\gamma < 2$:

$$\frac{\partial^\gamma C(x,t)}{\partial t^\gamma} + \frac{\partial C(x,t)}{\partial t} = -\frac{\partial C(x,t)}{\partial x} + \frac{\partial^2 C(x,t)}{\partial x^2} + f(x,t), \tag{55}$$

We take $f(x,t) = 3\left[t^2 + 2t^{2-\gamma}/\Gamma(3-\gamma)\right] e^x$, and the initial and boundary conditions are given by

$$\begin{cases} C(x,0) = 0, \quad C_t(x,0) = 0, \quad 0 < x < 1, \\ C(0,t) = t^3, \quad C(1,t) = t^3 e, \quad 0 \le t \le 1. \end{cases} \tag{56}$$

where $\gamma = 1.85$. The exact solution of the equation is $u(x,t) = t^3 e^x$.

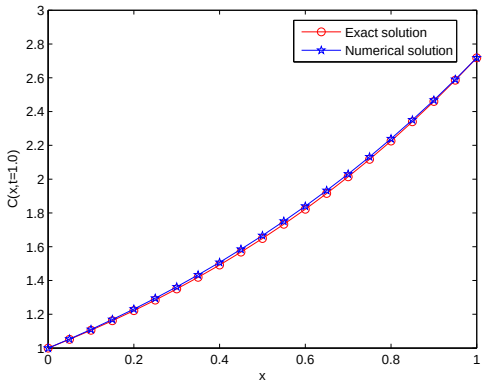

Fig. 18. Comparison between the exact solution and the numerical solution when $T = 1$ with $\gamma = 1.85$ in Example 7.

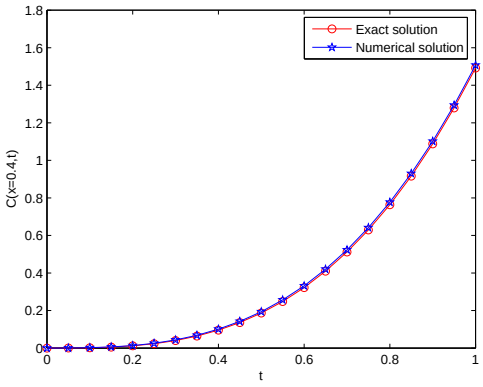

Fig. 19. Comparison between the exact solution and the numerical solution at $x = 0.4$with $\gamma = 1.85$ in Example 7.

Comparison between the exact and the numerical solutions are shown in Figs. 18 and 19. From Figs. 18 and 19, it can be seen that the numerical solution is in excellent agreement with the exact solution.

Example 8 (Model 5):

Consider the following time fractional advection-diffusion-wave model with damping with index $1 < \gamma < 2$

$$\frac{\partial^\gamma C(x,t)}{\partial t^\gamma} + \frac{\partial C(x,t)}{\partial t} = -\frac{\partial C(x,t)}{\partial x} + \frac{\partial^2 C(x,t)}{\partial x^2}, \tag{57}$$

with the initial and boundary conditions given by

$$\begin{cases} C(x,0) = \delta(x), \frac{\partial C(x,0)}{\partial t} = \delta(x) \quad 0 \le x \le b, \\ C(0,t) = 0, \quad \frac{\partial C(b,t)}{\partial x} = 0, \quad 0 < t \le T. \end{cases} \tag{58}$$

The computational results for different γ at $T = 20$ and $x = 26$ are shown in Figs. 20 and Fig. 21, respectively.

7 Conclusions

In this paper, some effective numerical methods for solving a class of fractional advection-dispersion models have been described and demonstrated. The stability and convergence of the implicit numerical methods are analysed systematically. Finally, some results are given to demonstrate the effectiveness of theoretical analysis. These equations can be used to simulate the regional-scale anomalous dispersion with heavy tails. The methods and techniques discussed

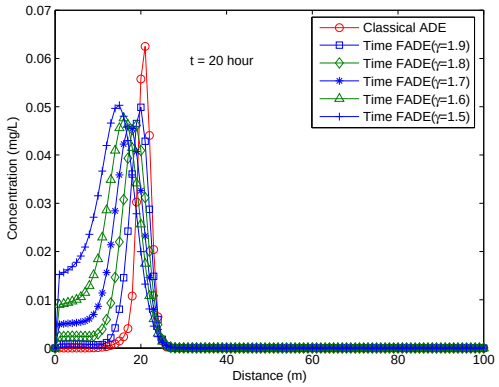

Fig. 20. The snapshot of tracers whose transport is governed by the time FADE (57) and (58) when $T = 20$.

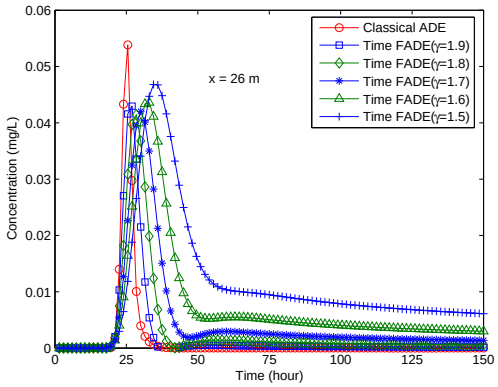

Fig. 21. The snapshot of tracers whose transport is governed by the time FADE (57) and (58) when $x = 26$.

in this paper can also be applied to solve other kinds of fractional partial differential equations.

Acknowledgements

This research has been supported by the Australian Research Council grant entitled "A Grid based platform for multi-scaled biological simulation" D-P1094333.

References

[1] E.E. Adams and L.W. Gelhar, Field study of dispersion in a heterogeneous aquifer: 2. Spatial moment analysis. Water Resources Researces, 28(12)(1992), 3293–3307.

[2] P. Becker-Kern, M.M. Meerschaert and H.P. Scheffler, Limit theorem for continuous time random walks with two time scales. Journal Applled Probability, 41(2004), 455–466.

[3] D.A. Benson, S.W. Wheatcraft, M.M. Meerschaert, Application of a fractional advection-dispersion equation, Water Resources Researces, 36(6)(2000), 1403–1412.

[4] D.A. Benson, S.W. Wheatcraft, M.M. Meerschaert, The fractional-order governing equation of Levy motion, Water Resources Researces, 36 (6) (2000), 1413–1423.

[5] J.P. Bouchaud, A. Georges, Anomalous diffusion in disordered media: statistical mechanisms, models and physical applications, Physics Reports (Review Section of Physics Letters), 195(4-5)(1990), 127–293.

[6] J. Eggleston and S. Rojstaczer, Identification of large-scale hydraulic conductivity trends and the influence of trends on contaminant transport, Water Resources Researces, 34(9)(1998), 2155–2168.

[7] R. Lin and F. Liu, Fractional high order methods for the nonlinear fractional ordinary differential equation, Nonlinear Analysis, 66(2007), 856–869.

[8] F. Liu, V. Anh and I. Turner, Numerical Solution of the Space Fractional Fokker-Planck Equation, Journal of Computational and Applied Mathematics, 166(2004), 209–219.

[9] F. Liu, P. Zhuang, V. Anh, I. Turner and K. Burrage , Stability and Convergence of the difference Methods for the space-time fractional advection-diffusion equation, Applied Mathematics and Computation, 91(2007), 12–20.

[10] E. Major, D. A. Benson, J. Revielle, H. Ibrahim, A. M. Dean, R. M. Maxwell, E. P. Poeter, and M. Dogan , Comparison of Fickian and temporally non-local transport theories over many scales in an exhaustively sampled sandstone slab, Water Resource Research, 47(2011), W10519, doi:10.1029/2011WR010857.

[11] F. Mainardi, Fraction calculus: some basic problems in continuum and statistical mechanics (A. Carpinteri, F. Mainardi, Eds.), Fractal and Fractional Calin Continuum Mechanics, Springer, Wien, (1997), 291-348.

[12] F. Mainardi, Y. Luchko, G. Pagnini, The fundamental solution of the space-time fractional diffusion equation, Fractional Calculus and Applied Analysis, 4 (2001), 153-1925.

[13] M.M. Meerschaert and C. Tadjeran, Finite difference approximations for two-sided space-fractional partial differential equations, Applied numerical mathematics, 56(2006), 80–90.

[14] M.M. Meerschaert and H.P. Scheffler, Limit theorems for continuous time random walks with infinite mean waiting times, Journal Applled Probability, 41(3)(2004), 623–638.

[15] K.B. Oldham and J. Spanier, The Fractional Calculus, Academic Press, New York, 1974.

[16] I. Podlubny, Fractional Differential Equations, Academic Press, New York, 1999.

[17] I. Podlubny, Matrix approach to discrete fractional calculus, Fractional Calculus and Applied Analysis, vol. 3, no. 4(2000), 359–386, http://people.tuke.sk/igor.podlubny/pspdf/ma2dfc.pdf).

[18] I. Podlubny, A. Chechkin, T. Skovranek, YQ. Chen, B. M. Vinagre Jara, Matrix approach to discrete fractional calculus II: partial fractional differential equations, Journal of Computational Physics, vol. 228, no. 8(2009), 313-7-3153, http://dx.doi.org/10.1016/j.jcp.2009.01.014 (preprint: http://arxiv.org/abs/0811.1355).

[19] H. Risken, The Fokker-Planck Equation, Springer, Berlin, 1988.

[20] R. Schumer, D.A. Benson, M.M Meerschaert and B. Baeumer, Fractal mobile/immobile solute transport, Water Resources Researces, 39(10)(2003), 1296.

[21] Q. Yang, F. Liu and I. Turner. Numerical methods for fractional partial differential equations with Riesz space fractional derivatives. Applied Mathematical Modelling, 34(1)(2010), 200–218.

[22] Y. Zhang, D.A. Benson, M.M. Meerschaert, and H.P. Scheffler, On Using Random Walks to Solve the Space-Fractional Advection-Dispersion Equations, Journal of Statistical Physics, Vol. 123, No. 1(2006), 89.

[23] Y. Zhang, D.A. Benson and D.M. Reeves, Time and space nonlocalities underlying fractional-derivative models: Distinction and literature review of field applications, Advances in Water Resources , 32(2009),561–581.